Nonsteady state carbon sequestration in forest ecosystems of China estimated by data assimilation

Tao Zhou,[1] Peijun Shi,[1] Gensuo Jia,[2] and Yiqi Luo[3]

[1]   Carbon sequestration occurs only when terrestrial ecosystems are at nonsteady states. Despite of their ubiquity in the real world, the nonsteady states of ecosystems have not been well quantified, especially at regional and global scales. In this study, we developed a two-step data assimilation scheme to estimate carbon sink strength in China's forest ecosystems. Specifically, the two-step scheme consists of a steady state step and a nonsteady state step. In the steady state step, we constrained a process-based model (Terrestrial Ecosystem Regional (TECO-R) model) against biometric data (net primary production NPP, biomass, litter, and soil organic carbon) in mature forests. With a subset of the parameter values estimated from the steady state data assimilation being fixed, the nonsteady state data assimilation was performed to estimate carbon sequestration in China's forest ecosystems. Our results indicated that 17 out of the 22 total parameters in the TECO-R model were well constrained by the biometric data with the steady state data assimilation. When observations from both mature and developing forests were used, all the 10 parameters related to carbon sequestration in vegetation and soil carbon pools were well constrained at the nonsteady state step. The estimated mean vegetation carbon sink in China's forests is $89.7 \pm 16.8\,\mathrm{gC\,m^{-2}\,yr^{-1}}$, comparable with the values estimated from the forest inventory and other process-based regional models. The estimated mean soil and litter carbon sinks in China's forests are 14.1 ± 20.7 and $4.7 \pm 6.5\,\mathrm{gC\,m^{-2}\,yr^{-1}}$. This study demonstrated that a two-step data assimilation scheme can be a potent tool to estimate regional carbon sequestration in nonsteady state ecosystems.

1.   Introduction

[2]   Forest ecosystems have been identified as a large and persistent carbon sink [*Pan et al.*, 2011a] and play a significant role in the mitigation of climate change caused by anthropogenically emitted carbon dioxide [*Intergovernmental Panel on Climate Change*, 2007]. Although research on the global carbon budget indicated that the terrestrial ecosystem is a huge carbon sink and could significantly regulate carbon-climate interactions, its magnitude, spatial patterns, and trends are still not well quantified [*Ballantyne et al.*, 2012; *Liu*, 2009; *Pan et al.*, 2011a; *Sarmiento et al.*, 2010]. It is imperative to develop new methods to identify the magnitude and spatial pattern of the terrestrial carbon sink to constrain the modern global carbon budget and better simulate future carbon-climate interactions.

[3]   Various methods have been used to estimate terrestrial carbon sinks, but each has some pros and cons. The process-based carbon cycle models simulate the magnitude of carbon sinks as affected by different factors such as CO_2 fertilization, climate change, and disturbances [*Tian et al.*, 2011; *Williams et al.*, 2012]. However, at the regional and global scales, the carbon sinks modeled in this way still have high uncertainties [*Piao et al.*, 2009]. Spatially explicit remote sensing offers an important data source for regional carbon cycle research, revealing vegetation dynamics and spatial patterns [*Piao et al.*, 2005], but it provides limited information on the carbon cycle of soil. The forest inventory method quantifies changes in biomass stock, which can be used for carbon sink estimation at national scale [*Fang et al.*, 2007; *Pan et al.*, 2011a; *Williams et al.*, 2012]. However, this approach only measures the timber volume instead of vegetation and soil carbon pools [*Fang et al.*, 2007]. In addition, the inventory approach is ridiculously labor intensive and could not be practiced everywhere. Eddy-flux measurement of net ecosystem exchange (NEE) directly quantifies carbon sinks or sources in ecosystems [*Baldocchi et al.*, 2001]. However, the number of NEE observation sites is quite small relative to the high spatial heterogeneity of terrestrial ecosystems [*Xiao et al.*, 2011]. The method offers no information

[1]State Key Laboratory of Earth Surface Processes and Resource Ecology, Beijing Normal University, Beijing, China.
[2]TEA, Institute of Atmospheric Physics, Chinese Academy of Sciences, Beijing, China.
[3]Department of Microbiology and Plant Biology, University of Oklahoma, Norman, Oklahoma, USA.

Corresponding author: T. Zhou, State Key Laboratory of Earth Surface Processes and Resource Ecology, Beijing Normal University, No.19 Xinjiekouwai St., Beijing 100875, China. (tzhou@bnu.edu.cn)
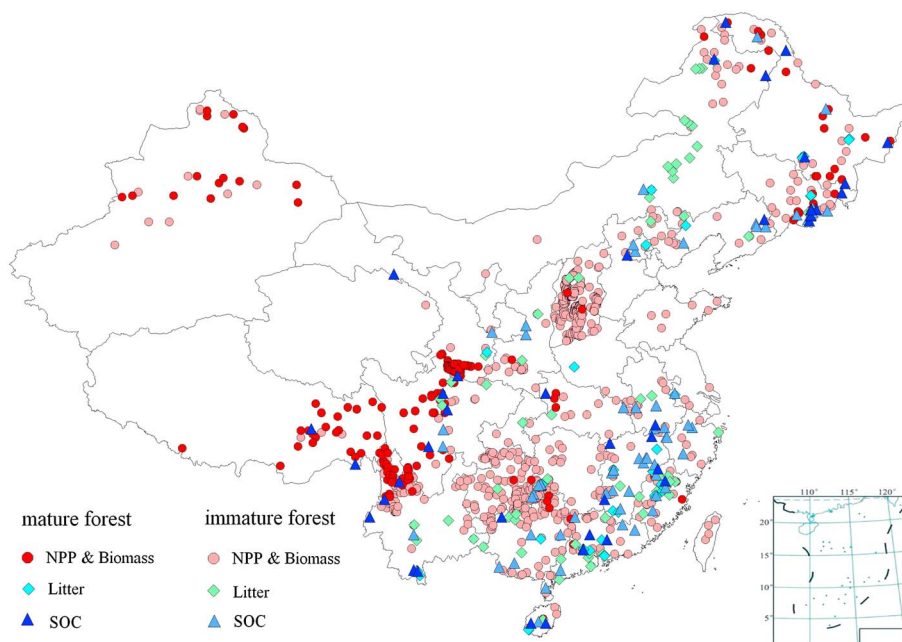
Figure 1. Spatial locations of the observed data used for parameter estimation.

on carbon sinks for specific carbon pools, either. Biometric observations of NPP, biomass, litter, and soil organic carbon have been widely available in most ecosystems. However, these observations only contain partial information related to the net exchange between the ecosystem and the atmosphere, and therefore cannot be used to directly estimate regional carbon sink.

[4] The data assimilation method is an effective approach to quantifying the dynamic disequilibrium of the terrestrial carbon cycle (i.e., the magnitude of disequilibrium in carbon cycle varies with time), as it assimilates multiple sources of information from field observations and process-based models [*Luo et al.*, 2011]. At a given site with an abundance of observation data sets, the process-based model can directly simulate the disequilibrium by forward modeling using optimal model parameters and observed initial values [*Luo et al.*, 2003], or inversely estimated initial carbon pools and the magnitude of disequilibrium from observed time series data sets [e.g., *White and Luo*, 2002; *Weng and Luo*, 2011]. The magnitudes of disequilibrium significantly impact the modeled carbon pools and their dynamic variation [*Carvalhais et al.*, 2008, 2010a], so the magnitude of disequilibrium can be inversely estimated from the observations of time series.

[5] For regional and global scales, however, neither observations of initial carbon pools nor observations of time series are available for most spatial grids of land models. That is, the methods of estimating the magnitude of disequilibrium at individual ecosystem sites are no longer valid for the regional scale. As a result, nearly all regional or global models have to spin-up their models to a steady state to estimate the initial values of carbon pools before predicting the magnitude of disequilibrium [*Carvalhais et al.*, 2010a; *Friedlingstein et al.*, 2006; *Xia et al.*, 2012]. At regional scales, data assimilation is usually used to estimate the optimal model parameters and the initial state under the steady state assumption [*Barrett*, 2002; *Zhou and Luo*, 2008]. Up to now, few studies

were ever published using the data assimilation method to directly estimate nonsteady state carbon sinks at regional and global scales. In the regional models, parameters to be optimized were usually based on plant functional type, and the observations from multisites were used as constrains to estimate a single set of optimal parameters [*Kuppel et al.*, 2012]. However, some recent studies considered more factors for grid-specific parameters, such as the similarities of climatic and phonological conditions [*Carvalhais et al.*, 2010b].

[6] This study aims to estimate nonsteady state regional forest carbon sinks in China directly from the large amounts of biometric observations of NPP, biomass, litter, and soil organic carbon (SOC) with supplementary driving data from spatially explicit remote sensing observations. We used a two-step data-model fusion scheme for parameter estimation. The first step is for parameter estimation at steady state using the observations only from mature forest sites. The second step is for the estimation of carbon sink parameters at nonsteady state using all observed data combined with the optimal parameters retrieved in the first step.

2. Methods and Data

2.1. Data

[7] This study used 12 observed data sets, including three NPP data sets [*Luo*, 1996] (i.e., NPP in leaves, stems, and roots) containing 1172 data points each; five biomass data sets [*Luo*, 1996] (i.e., biomass of leaves, stems, and roots in three soil layers) containing 1172 data points each; a litter data set containing 330 data points collected from field observations reported in the literature; and three SOC data sets for the three soil layers [*Wang et al.*, 2003], each containing 129 data points. The spatial distribution of those observed data points is illustrated in Figure 1. Among these observations, the sites of mature forest (i.e., forests older than 100 years or
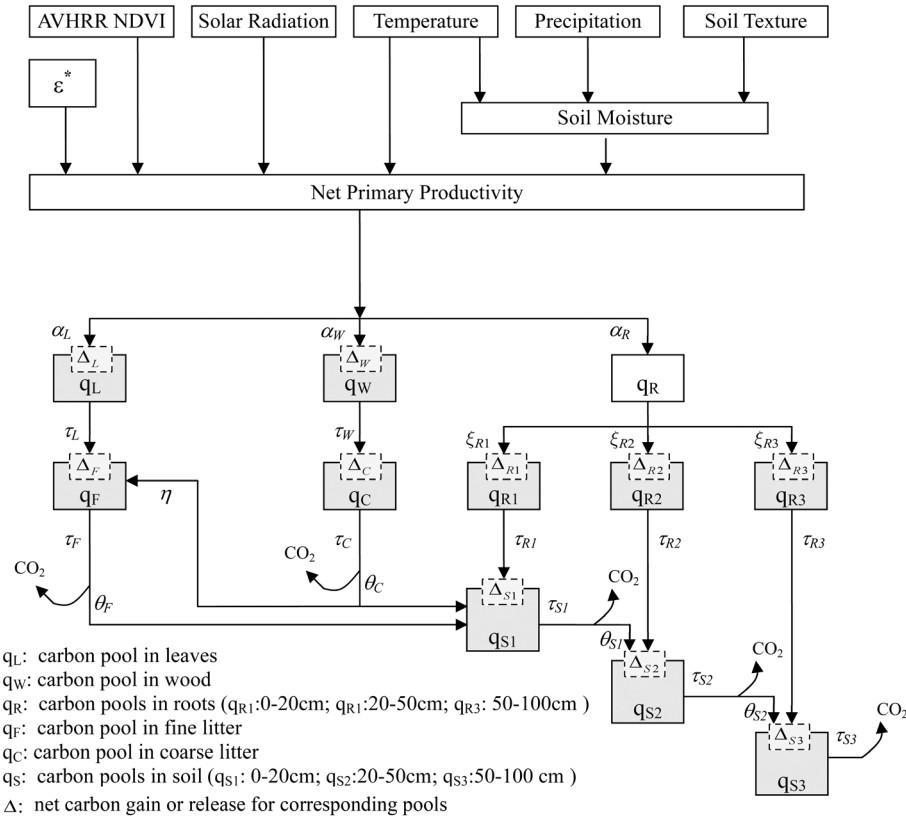
Figure 2. The structure of the Terrestrial Ecosystem Regional (TECO-R) model and its key parameters. For the steady state, the parameters of net carbon gain/release equal zeros. For the nonsteady state, the parameters of carbon gain/release were used only for diagnostic analysis, which aimed to estimate the carbon pools at nonsteady state. In addition, the parameters of carbon gain/release are not free variables that dependent completely on their input and output based on conservation of mass.

forests indicated in the literature as mature forests) were used for the first step of the parameter estimation at steady state.

[8] In addition to the biometric data sets, this study uses spatially explicit remote sensing and geographic information system (GIS) data sets, including (1) the advanced very high resolution radiometer–normalized difference vegetation index (NDVI) continental subsets of 8 km spatial resolution from 1982 to 2000 available from the Global Inventory Modeling and Mapping Studies (http://glcf.umiacs.umd.edu/); (2) GIS data sets of monthly solar radiation, temperature, and precipitation from the China Meteorological Data Sharing Service System (http://cdc.cma.gov.cn); (3) a 1:1400 M soil texture map of China; and (4) a 1:400 M vegetation map of China available from Data Sharing Infrastructure of Earth System Science (http://www.geodata.cn), from which the map of forest types in this study was produced [*Dai et al.*, 2011]. All those auxiliary data sets were resampled to a common Geographic (Latitude/Longitude) projection and spatial resolution (0.08°) using Bilinear Interpolation in ERDAS IMAGINE software. Considering the discrepancies in sampling time among different ground-based observations and the influences of interannual variability of climate factors and NDVI on the modeling of NPP and biomass, the NDVI and climate factor values used for the parameter estimation were multiyear monthly means from 1982 to 2000 (i.e., the means of the monthly data for the period from 1982 to 2000) to match with the field observation data sets. The model simulates the monthly NPP using the monthly NDVI and climate data, and then summed to yearly total NPP before parameters estimation.

2.2. Model

[9] The process-based Terrestrial Ecosystem Regional model (TECO-R) [*Zhou and Luo*, 2008; *Zhou et al.*, 2010] was used in the data assimilation to synthesize information in the model, field observations, and spatially explicit satellite data (Figure 2 and Table 1). The TECO-R model contains three sequential submodels that determine ecosystem carbon input (i.e., net primary production), the carbon allocation of NPP to different vegetation carbon pools (i.e., leaves, stems, and roots), and the decomposition of the litter and soil organic carbon (see Appendix A).

[10] TECO-R uses a light-use efficiency (LUE) scheme of Carnegie-Ames-Stanford Approach (CASA) model [*Field et al.*, 1995; *Potter et al.*, 1993] to simulate the spatially specific NPP pattern at regional scale. The NPP is determined by satellite-based normalized difference vegetation index (NDVI) and climate driving factors. The parameter of potential maximum light-use efficiency (ε^*) is related to the vegetation type and is typically characterized under optimal environmental conditions for specific vegetation types [*Zhang et al.*, 2012; *Zhao and Running*, 2010]. In our diagnostic TECO-R model, the NPP is derived from NDVI, radiation, and light-use efficiency; and, as carbon input of ecosystem, acts as a driver of the ecosystem carbon cycle.

Table 1. Symbols and Definitions of Parameters and the Lower and Upper Limits[a]

Symbol	Definition	Unit	Lower Limit	Upper Limit
$\varepsilon*$	Maximum light-use efficiency	$gC\,MJ^{-1}$	0.0	2.76
α_L	Allocation of NPP to leaves	Dimensionless	0.0	1.0
α_W	Allocation of NPP to wood	Dimensionless	0.0	1.0
α_R	Allocation of NPP to roots	Dimensionless	0.0	1.0
ξ_{R1}	Allocation proportion of NPP for roots (0–20 cm)	Dimensionless	0.0	1.0
ξ_{R2}	Allocation proportion of NPP for roots (20–50 cm)	Dimensionless	0.0	1.0
ξ_{R3}	Allocation proportion of NPP for roots (50–100 cm)	Dimensionless	0.0	1.0
θ_F	Carbon partitioning coefficient of the fine litter pool	Dimensionless	0.0	0.5
θ_C	Carbon partitioning coefficient of coarse litter pool	Dimensionless	0.0	0.5
θ_{S1}	Carbon partitioning coefficient of SOC (0–20 cm)	Dimensionless	0.0	0.1
θ_{S2}	Carbon partitioning coefficient of SOC (20–50 cm)	Dimensionless	0.0	0.1
η	Fraction of mechanical breakdown for coarse litter pool	Dimensionless	0.0	0.1
τ_L	Biome-specific carbon residence time of leaves	Year	0.0	10.0
τ_W	Biome-specific carbon residence time of wood	Year	0.0	500.0
τ_{R1}	Biome-specific carbon residence time of roots (0–20 cm)	Year	0.0	10.0
τ_{R2}	Biome-specific carbon residence time of roots (20–50 cm)	Year	0.0	20.0
τ_{R3}	Biome-specific carbon residence time of roots (50–100 cm)	Year	0.0	50.0
τ_F^*	Baseline residence time of fine litter	Year	0.0	10.0
τ_C^*	Baseline residence time of coarse litter	Year	0.0	50.0
τ_{S1}^*	Baseline residence time of SOC (0–20 cm)	Year	0.0	100.0
τ_{S2}^*	Baseline residence time of SOC (20–50 cm)	Year	0.0	250.0
τ_{S3}^*	Baseline residence time of SOC (50–100 cm)	Year	0.0	500.0
Δ_L	Net carbon gain or release for leaf pool	$gC\,m^{-2}\,yr^{-1}$	−200	200
Δ_W	Net carbon gain or release for wood pool	$gC\,m^{-2}\,yr^{-1}$	−1000	1000
Δ_{R1}	Net carbon gain or release for roots (0–20 cm)	$gC\,m^{-2}\,yr^{-1}$	−200	200
Δ_{R2}	Net carbon gain or release for roots (20–50 cm)	$gC\,m^{-2}\,yr^{-1}$	−200	200
Δ_{R3}	Net carbon gain or release for roots (50–100 cm)	$gC\,m^{-2}\,yr^{-1}$	−200	200
Δ_F	Net carbon gain or release for fine litter pool	$gC\,m^{-2}\,yr^{-1}$	−200	200
Δ_C	Net carbon gain or release for coarse litter pool	$gC\,m^{-2}\,yr^{-1}$	−200	200
Δ_{S1}	Net carbon gain or release for SOC pool (0–20 cm)	$gC\,m^{-2}\,yr^{-1}$	−500	500
Δ_{S2}	Net carbon gain or release for SOC pool (20–50 cm)	$gC\,m^{-2}\,yr^{-1}$	−500	500
Δ_{S3}	Net carbon gain or release for SOC pool (50–100 cm)	$gC\,m^{-2}\,yr^{-1}$	−500	500

[a]Sixteen parameters were biome-specific, including one maximum light-use efficiency, 10 baseline carbon residence, and five related carbon partition coefficients. Six NPP allocation coefficients and 10 carbon gain/loss parameters were dependent on both the biome type and age.

[11] The estimated NPP is allocated to different vegetation carbon pools (leaves, stem, and roots) based on NPP allocation coefficients (α_L, α_W, α_R, ξ_{R1}, ξ_{R2}, and ξ_{R3}) (see Appendix B). Then, the carbon enters into carbon pools of the litter and soil organic carbon and is finally released from the ecosystem though heterotrophic respiration. As the carbon efflux from a certain carbon pool is determined by its residence time (i.e., τ_L, τ_W, τ_{R1}, τ_{R2}, τ_{R3}, τ_F, τ_C, τ_{S1}, τ_{S2}, and τ_{S3}), the storage and change for each carbon pool is jointly determined by its carbon input, which is controlled by the NPP and the allocation coefficients, and carbon output, which is controlled by carbon residence times.

[12] When the carbon cycle of an ecosystem is at steady state, the magnitudes of the carbon pools in Figure 2 are completely determined by carbon input (i.e., the NPP) and residence time [*Xia et al.*, 2013, see Appendix C]. In this situation, when the observations are obtained from mature forests, in which the carbon cycle is assumed to be in equilibrium and the parameters related to carbon disequilibrium can be omitted, then the parameters related to carbon residence time can be effectively estimated through inverse algorithms [*Barrett*, 2002; *Zhou et al.*, 2010].

[13] When the carbon cycle of an ecosystem is not at steady state, usually for forest sites that have experienced a disturbance or are relatively young [*Luo and Weng*, 2011; *Pan et al.*, 2011b; *Yang et al.*, 2011], the carbon input for vegetation pools and the subsequent litter and SOC pools no longer equal their carbon output. Variations in carbon input occur for two reasons. One is the change in total production (NPP), which

can be monitored through remote sensing-based NDVI and the light-use efficiency model. The other is a change in the NPP allocation to different vegetation pools, which is related with forest age and environmental conditions and can be inversely estimated through large sample of sites observations.

[14] In a nonsteady state, the carbon inputs and outputs are not equal, so the modeled carbon pools based only on the parameters estimated at a steady state do not agree with the values observed in the field. As a result, additional information (i.e., the magnitude of the carbon disequilibrium in each of the carbon pools) is necessary to accurately model the values of carbon pools [*Luo and Weng*, 2011]. In particular, if we relax the assumption on the equilibrium conditions (i.e., the carbon sink for each pool equals zero) and treat the magnitude of disequilibrium as adjustable model parameters, these parameter values can be optimally estimated using an inverse algorithm from the deviation between modeled (see Appendix D) and observed pool and flux values.

[15] Considering the fact that most sites only have subsets of data on NPP biomass and SOC, i.e., a site that has NPP and biomass observation but that lack SOC observations, and vice versa (Figure 1), they certainly do not have complete information to match all parts of modeled production, allocation, and decomposition in TECO-R. Therefore, it is impossible to estimate the carbon sink for each site based only on discrete observations. Fortunately, with the support of spatially related remote sensing data and data assimilation technology, those spatially dispersed observations on vegetation and soil can be pooled together to form an integrated
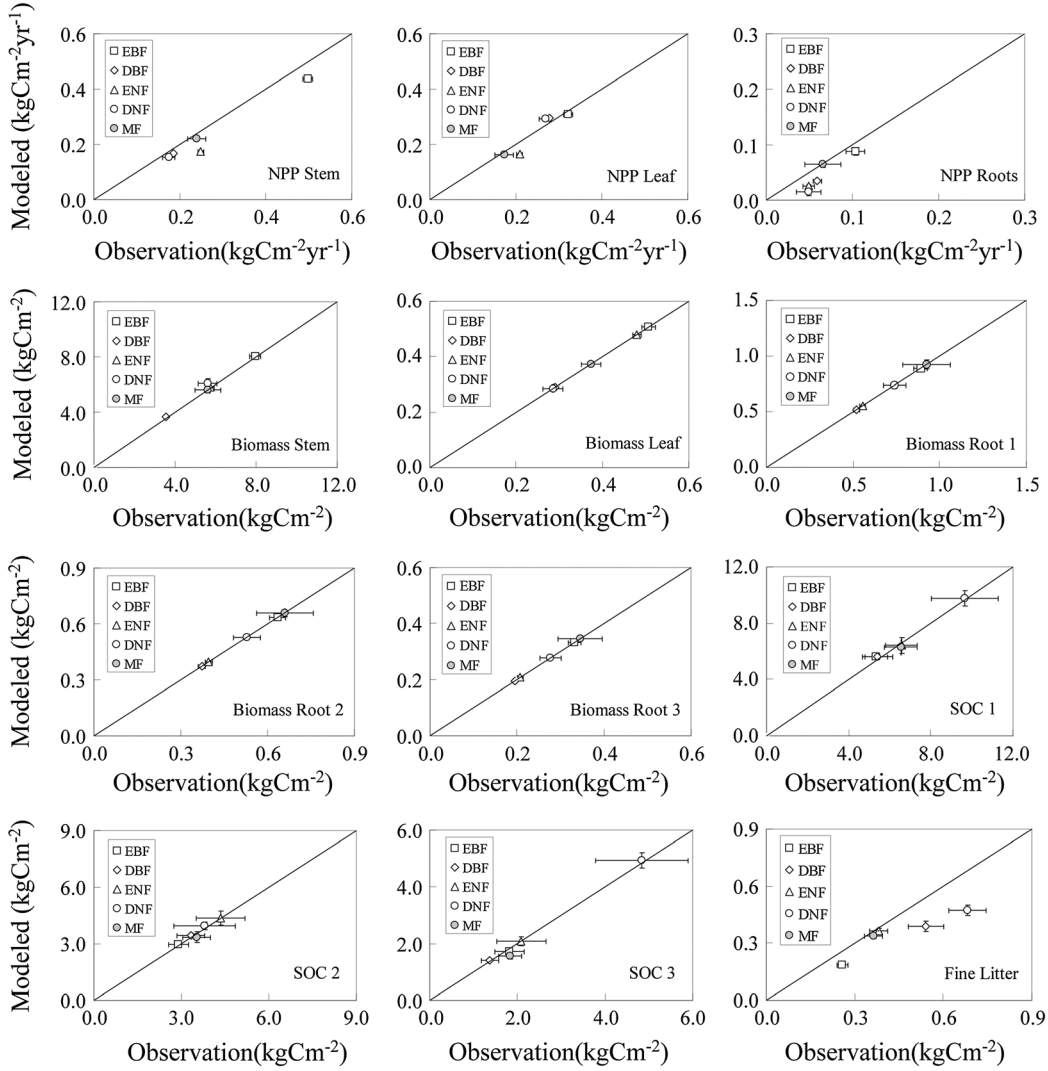
Figure 3. Comparisons between observed and modeled values. EBF: evergreen broadleaf forest; DBF: deciduous broadleaf forest; ENF: evergreen needleleaf forest; DNF: deciduous needleleaf forest; and MF: mixed forest.

information that reflects the regional mean value of the carbon sink.

2.3. Parameter Estimation

[16] In this study, we applied a two-step scheme to estimate the regional means of carbon sink parameters from a large database of biometrical observations (Figure 1). The first step is to estimate 22 model parameters at steady state using data only from the mature forest sites. The second step is to use all observations, including both mature and immature sites, to estimate 10 carbon sink parameters (i. e., Δ_L, Δ_W, Δ_{R1}, Δ_{R2}, Δ_{R3}, Δ_C, Δ_F, Δ_{S1}, Δ_{S2}, and Δ_{S3}) and six related NPP allocation parameters (i. e., α_L, α_W, α_R, ξ_{R1}, ξ_{R2}, and ξ_{R3}) that usually vary with forest age while parameters related to the baseline carbon residence times retrieved in the first step were fixed.

[17] The parameter estimation was based on the weighted least squares principle that minimizes the deviations between the modeled and observed values of all 12 data sets for each of five forest types, which included evergreen broadleaf forest (EBF), deciduous broadleaf forest (DBF), evergreen needleleaf forest (ENF), deciduous needleleaf forest (DNF), and mixed forest (MF). To estimate the globally optimal parameters, this study used a genetic algorithm (GA) [*Zhou and Luo*, 2008]. We ran the optimization algorithm 500 times for each forest type to obtain its mean and standard deviation of the estimated parameters. As the observation data sets used to parameter estimation were completely same for each run, so the main sources of uncertainty were caused by the inverse modeling algorithm. That is, the uncertainty originated from the combinations of parameter values that yield equally good fits between the model and the data [*Barrett*, 2002; *Fox et al.*, 2009; *Wang et al.*, 2009].

[18] In addition to inverse modeling algorithm, the uncertainty of estimated regional means of carbon sink is also related with the sampling error (i.e., the uncertainty caused by different samples of observation). In this study, we used a bootstrap method [*Wilks*, 2006] to resample the observational data 500 times and then estimated the optimal parameters and uncertainties.
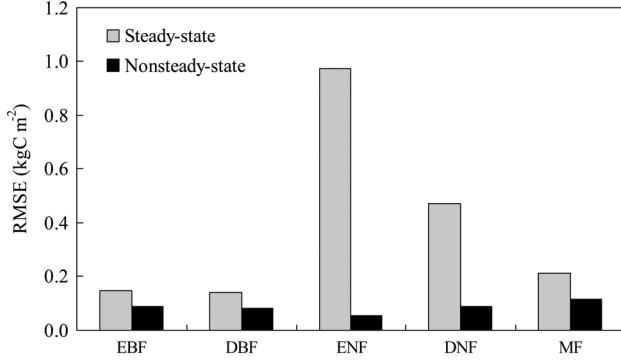
Figure 4. Comparisons of the root-mean-square error between the steady and nonsteady state.

2.4. Parameter Estimation at Steady State

[19] Given the site observations of the mature forest, we defined a partial cost function j_m as the sum of squares of deviations between observed and modeled values for data set m:

$$j_m = \sum_{n=1}^{N_m} [y_{nm} - \hat{y}_{nm}(x_n, \mathbf{a})]^2 \qquad (1)$$

where y_{nm} is the nth observed data point in the mth data set; $\hat{y}_{nm}(x_n; \mathbf{a})$ is the modeled value (see Appendix C) that corresponds to the observation y_{nm}; N_m is the total number of data points in the mth data set; x_n is an auxiliary forcing vector that includes NDVI, solar radiation, air temperature, precipitation, and soil texture, in a spatial grid where the nth observation was made; and $\mathbf{a}$ is a vector consisting of 22 parameters: $\mathbf{a} = \{\varepsilon^*, \alpha_L, \alpha_W, \alpha_R, \xi_{R1}, \xi_{R2}, \xi_{R3}, \tau_L, \tau_W, \theta_F, \theta_C, \eta, \tau_{R1}, \tau_{R2}, \tau_{R3}, \tau_F^*, \tau_C^*, \tau_{S1}^*, \tau_{S2}^*, \tau_{S3}^*, \theta_{S1}, \theta_{S2}\}$, where each of the parameters is defined in Table 1.

[20] One given data set may provide information to constrain a subset of parameters in vector $\mathbf{a}$. When all 12 data sets are used, all 22 parameters can be constrained to a certain degree. As a result, an integrated cost function J, which consists of M (=12) partial cost functions j_m, is defined to measure the deviations between modeled and observed values for all data points in the 12 data sets. Thus, the cost function J to be minimized is

$$J = \sum_{m=1}^{M} \lambda_m \left\{ \sum_{n=1}^{N_m} [y_{nm} - \hat{y}_{nm}(x_n, \mathbf{a})]^2 \right\}, \qquad m = 1, 2 \cdots M, \qquad (2)$$

where λ_m is a weighting factor of the partial cost j_m, which is inversely proportional to the variance of each data set [*Luo et al.*, 2003; *Zhou and Luo*, 2008]. The cost function J in equation 2 was applied to each of the five forest types so that five sets of forest-specific values of parameter vector $\mathbf{a}$ were obtained.

2.5. Parameter Estimation at Nonsteady State

[21] The estimation of the additional 10 carbon sink parameters and six nonsteady state allocation parameters was based on the large sample of all site observations. Thus, the partial cost function j'_m is defined as

$$j'_m = \sum_{n=1}^{N'_m} [y_{nm} - \hat{y}_{nm}(x_n, \mathbf{b}, \mathbf{a_0})]^2, \qquad (3)$$

where $\hat{y}_{nm}(x_n; \mathbf{b}, \mathbf{a_0})$ is the modeled value at nonsteady state (see Appendix D) that corresponds to the observation

y_{nm}. N'_m is the number of data points in the second step (i.e., nonsteady state); $\mathbf{b}$ is the set of 16 parameters that will be estimated, $\mathbf{b} = \{\Delta_L, \Delta_W, \Delta_{R1}, \Delta_{R2}, \Delta_{R3}, \Delta_C, \Delta_F, \Delta_{S1}, \Delta_{S2}, \Delta_{S3}, \alpha_L, \alpha_W, \alpha_R, \xi_{R1}, \xi_{R2}, \xi_{R3}\}$; $\mathbf{a_0}$ is the set of the parameters optimally retrieved in the first step, $\mathbf{a_0} = \left\{\varepsilon^*, \tau_L, \tau_W, \theta_F, \theta_C, \eta, \tau_{R_1}, \tau_{R_2}, \tau_{R_3}, \tau_F^*, \tau_C^*, \tau_{S_1}^*, \tau_{S_2}^*, \tau_{S_3}^*, \theta_{S_1}, \theta_{S_2}\right\}$. As the parameters in $\mathbf{a_0}$ mainly reflect intrinsic properties of vegetation and soil in each biome, we assume that these parameters are the same for both the steady and nonsteady states.

[22] Light-use efficiency (LUE) is an important parameter for modeling ecosystem production in light-use efficiency models. The site-specific LUE was commonly expressed by a theoretical potential value (maximum light-use efficiency), which either as a global invariant constant or as a biome-specific constants, and site-specific scalars of environmental stress such as temperatures and water shortages [*Yuan et al.*, 2007]. In this study, we assumed that the parameter of maximum light-use efficiency is a biome-specific constant that do not vary with forest age, and the impacts of forest development stages on NPP embodied in site-specific NDVI.

[23] Similarly to the first step at steady state, the cost function J' to be minimized at nonsteady state is the following:

$$J' = \sum_{m=1}^{M} \lambda'_m \left\{ \sum_{n=1}^{N'_m} [y_{nm} - \hat{y}_{nm}(x_n, \mathbf{b}, \mathbf{a_0})]^2 \right\}, \qquad m = 1, 2 \cdots M. \quad (4)$$

2.6. Sensitivity Analysis of Steady State Assumption on Parameter Estimation

[24] To evaluate possible impacts of nonsteady condition of mature forests on parameter estimation, we did some sensitivity analysis for evergreen broadleaf forest (EBF), in which we assume that (1) the mature forest was a carbon sink; (2) the magnitudes of the ecosystem total carbon sink were 0% (i.e., a steady state), 2.5%, 5.0%, 7.5%, and 10.0% of the NPP, respectively, for five scenarios (i.e., the annual carbon sink was 0, 23, 47, 70, and 94 gC m^{-2} yr^{-1}, respectively); and (3) the carbon sink for each pool was proportional to its carbon storage (i.e., the values of the carbon sink were known constants for all 10 pools). The carbon sink parameters were known in the sensitivity analysis, so their effects on the baseline residence times could be evaluated (the first step). Thus, the effects of the changed residence times on the carbon sink parameters could also be estimated (the second step).

3. Results

3.1. Comparisons Between Modeled and Observed Values

[25] The regional scale comparisons indicated that the modeled means of NPP, Biomass, litter, and SOC are well matched with the corresponding mean observations (Figure 3), which implies that the estimated optimal model parameters effectively reflect general regional characteristics of the carbon pools. The comparisons also imply that the different types of observations (i.e., NPP, biomass, or SOC) at different spatial locations could be linked together and jointly constrain the model parameters.
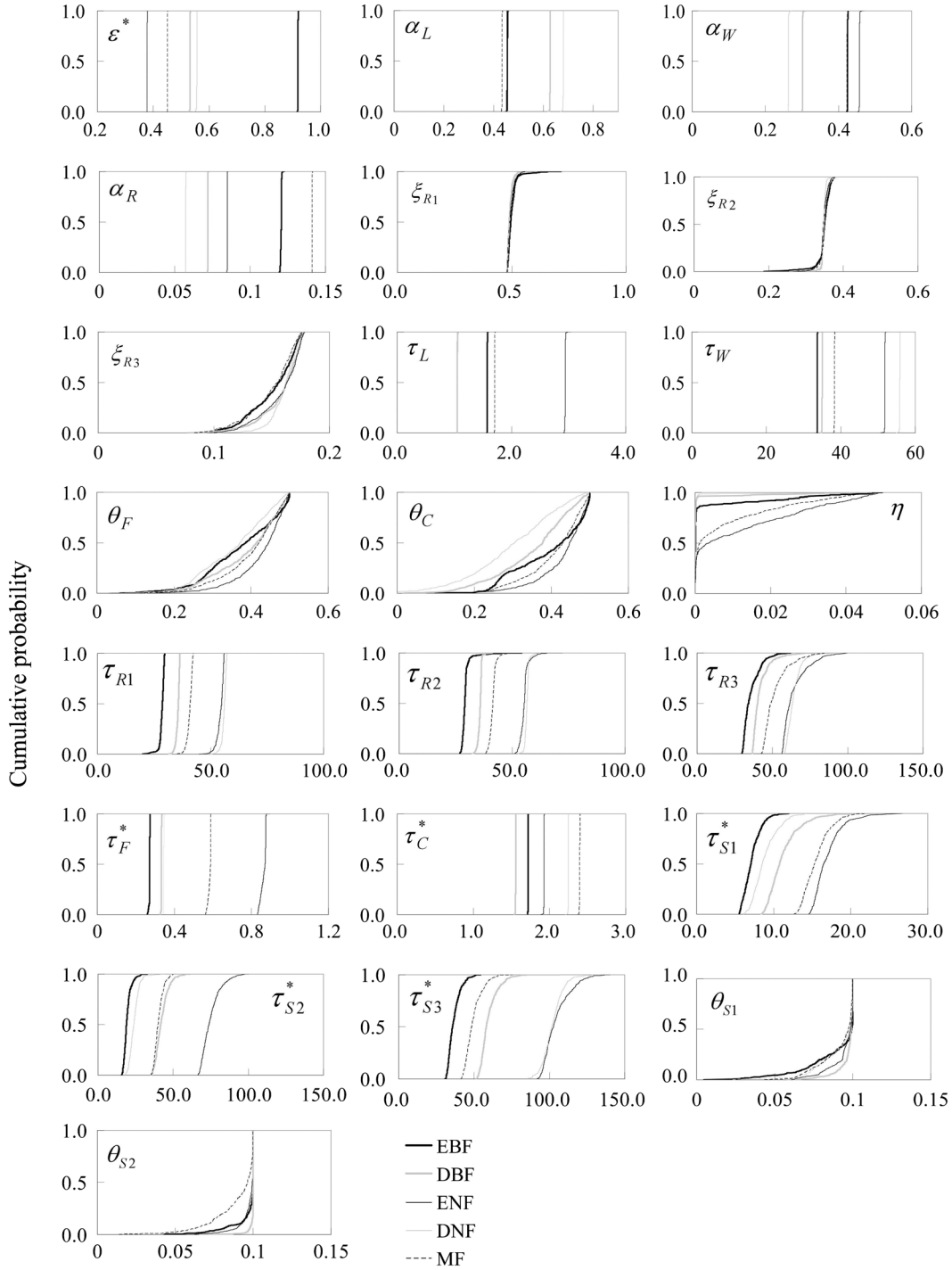
Figure 5. Optimal parameters at steady state estimated by 500 runs of a genetic algorithm.

[26] We applied a two-step data assimilation scheme in which the steady state assumption was relaxed to the nonsteady state in the second step. Thus, the carbon sink parameters are not necessary equal to zero and could be optimized based on field observations. As a result, the deviations between the modeled and observed values at the nonsteady state decrease significantly (Figure 4). The significant reduction in the root-mean-square error (RMSE) with the estimated carbon sink parameters is a benefit of the relaxation of the steady state assumption.

3.2. Optimal Model Parameters

[27] The parameters estimated at steady state for mature forest sites were shown in Figure 5. The results indicated that except five parameters related to carbon transfer among pools (i.e., θ_F, θ_C, η, θ_{S_1}, and θ_{S_2}), the other 17 parameters (i.e., ε^*, α_L, α_W, α_R, ξ_{R1}, ξ_{R2}, ξ_{R3}, τ_L, τ_W, τ_{R1}, τ_{R2}, τ_{R3}, τ_F^*, τ_C^*, τ_{S1}^*, τ_{S2}^*, and τ_{S3}^*), including 10 carbon residence time parameters, could be well constrained by the observations.

[28] All 10 carbon sink parameters (Δ_L, Δ_W, Δ_{R1}, Δ_{R2}, Δ_{R3}, Δ_C, Δ_F, Δ_{S1}, Δ_{S2}, and Δ_{S3}) were well constrained by the
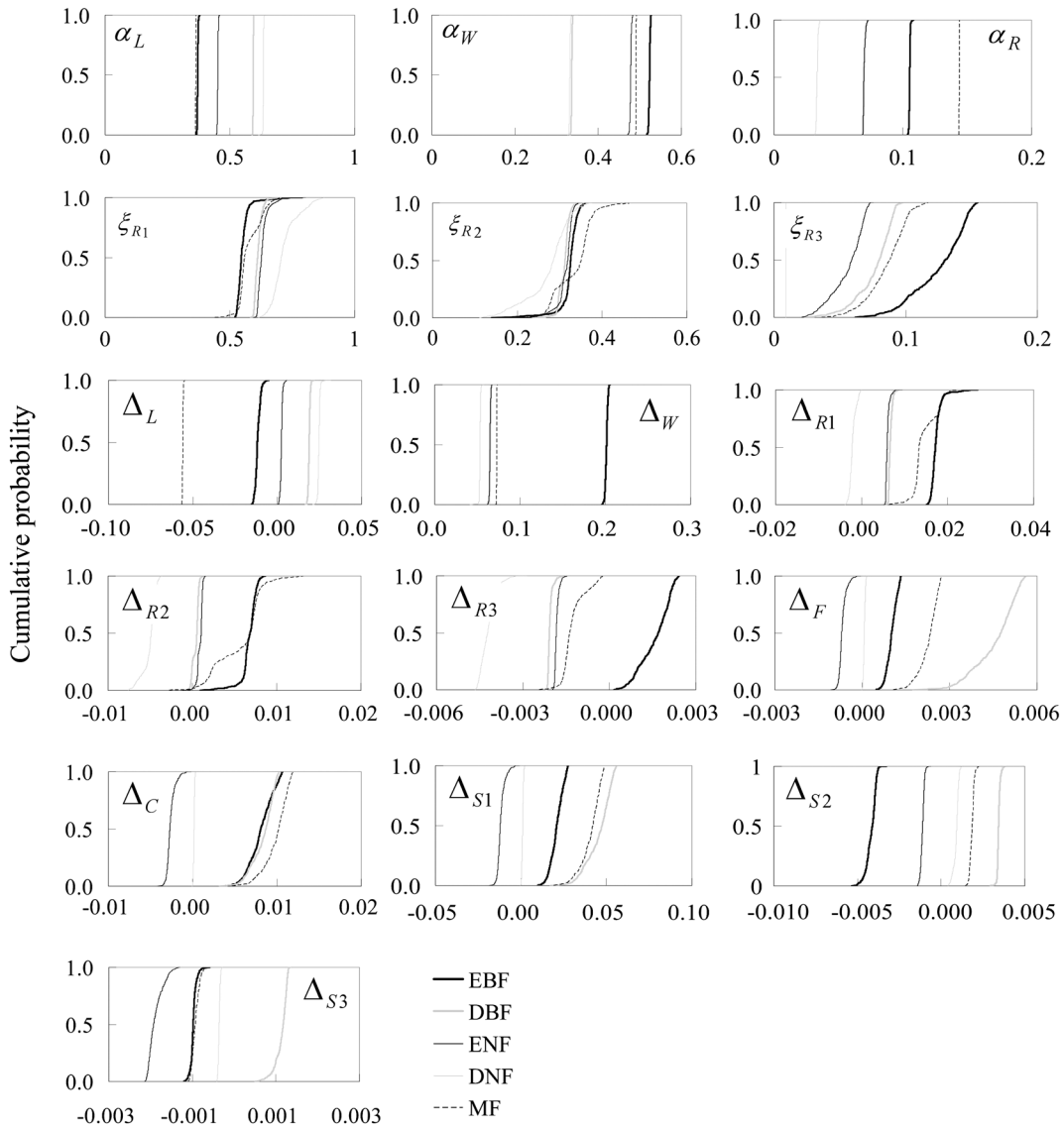
Figure 6. Optimal parameters at nonsteady state estimated by 500 runs of a genetic algorithm.

observation data, given the optimal carbon residence time parameters estimated at the preceding steady state step. Most of the estimated carbon sink parameters for five forests (Figure 6) are positive, indicating that their carbon inputs are larger than their outputs and that the ecosystems have a net carbon uptake.

[29] Although the parameters estimated at the first steady state step showed that five parameters could not be well constrained,

with optimal values located near the lower bound (η) or upper bound (θ_F, θ_C, θ_{S_1}, and θ_{S_2}), the results in Figure 6 indicate that these parameters do not affect the optimal estimations of carbon sink parameters in the second nonsteady state step. Consequently, equifinality exists for those parameters; each optimal parameter vector ($\theta_F, \theta_C, \eta, \theta_{S_1}$, and θ_{S_2}) estimated at the steady state has an equal impact on the estimation of the carbon sink parameters.

Table 2. Forest Carbon Sinks and Uncertainties for Vegetation, Soil, and Litter Carbon Pools

Forest Type	Area (10^6 ha)	Carbon Sink[a] (gC m^{-2} yr^{-1})							
		Vegetation		Soil		Litter		Total	
EBF	18.7	215.41	±19.30	15.75	±32.60	9.10	±14.90	240.26	±46.60
DBF	27.1	89.01	±11.10	50.10	±17.80	12.89	±6.60	152.00	±24.70
ENF	49.1	72.29	±8.20	−14.65	±19.10	−3.30	±4.50	54.34	±23.30
DNF	14.6	66.46	±46.00	1.55	±26.80	0.23	±6.20	68.24	±35.90
MF	21.1	36.20	±21.80	41.84	±13.10	12.20	±3.80	90.23	±25.40
All	130.6	89.74	±16.82	14.06	±20.65	4.73	±6.50	108.53	±28.67

[a]Mean ± SD; the standard deviation estimated from 500 bootstrap samples, which reflects uncertainties of both inverse modeling algorithm and sampling error.

Table 3. Vegetation Carbon Sink Estimated by Different Methods

Method	Period of Time	Area (10^6 ha)	Vegetation (TgC yr^-1)	Vegetation (gC m^-2 yr^-1)	Soil (gC m^-2 yr^-1)	Litter (gC m^-2 yr^-1)	Total (gC m^-2 yr^-1)	Ratio of Soil Sink (%)	Reference
Data assimilation	1982–2000	130.6	117.2±22.0	89.7±16.8	14.1±20.7	4.7±6.5	108.5±28.7	13.0	This study
Inventory	1982–1993	124–132	58.4±25.8	45.6±20.2					Fang et al. [2007]
Inventory	1994–2003	132–143	92.2±43.7	67.1±31.8					Fang et al. [2007]
Inventory	1990–1999	139.3	60	43.1	22.3	10.8[a]	76.2[a]	29.3	Pan et al. [2011a]
Inventory	2000–2007	155.6	115	73.9	18.0	5.1[a]	97.0[a]	18.6	Pan et al., [2011a]
Inventory	1999–2003	142.8	135.0	94.5					Lun et al. [2012]
Inventory and statistical model	1999–2003	142.8	210	147.1					Wang et al. [2010]
Inventory and site studies	1980s–1990s	108.6	68	62.6					Pan et al. [2004]
Process-based model (DLEM Dynamic Land Ecosystem Model)	1981–2000	126–137	82±18	61.3±12.7	12.0±7.6		73.3	16.4	Tian et al. [2011]
Process-based model (InTEC Integrated Terrestrial Ecosystem Carbon)	1988–2001	139		218.1	−46	−13.8	158.3	C source	Wang et al. [2011a]
Process-based model (FORCCHN Forest Ecosystem Carbon Budget Model for China)	1982–2002	130			−4.6			C source	Chen et al. [2008]
Process-based model	1982–1999	124.3	34	27.4					Li et al. [2009]
Inventory and remote sensing	1981–1999	127.9	19.5	15.2					Piao et al. [2005]
Empirical regression[b]	1982–1999	130			3.1±3.2				Piao et al. [2009]
Statistical estimation	1980–2000	249			4.7				Xie et al. [2007]

[a]Not including dead wood.
[b]Regression with annual temperature, precipitation, and NDVI/Biomass.

Table 4. Comparison of China's Forest Carbon Sink With Other Geographic Regions

Biome and Country/Region	Method	Period of Time	Area (10^6 ha)	Vegetation (TgC yr^-1)	Vegetation (gC m^-2 yr^-1)	Soil (gC m^-2 yr^-1)	Litter (gC m^-2 yr^-1)	Total (gC m^-2 yr^-1)	Ratio of Soil (%)	Ratio of Soil and Litter (%)	Reference
China's forests	Data assimilation	1982–2000	130.6	117.2	89.7	14.1	4.7	108.5	13.0	17.3	This study
Temperate forests	Inventory	1990–1999	733.6	345	47.0	21.8	6.3	75.1	29.0	37.4	Pan et al. [2011a]
Temperate forests	Inventory	2000–2007	766.7	454	59.2	20.3	5.9	85.4	23.8	30.7	Pan et al. [2011a]
Global forests	Inventory	1990–1999	3959.3	2991	75.5	12.6	4.2	92.3	13.7	18.2	Pan et al. [2011a]
Global forests	Inventory	2000–2007	3851.3	2941	76.4	11.8	4.1	92.3	12.8	17.2	Pan et al. [2011a]
Forests in U.S.	Inventory	1990–1999	245.7	118	48.0	3.7	4.9	56.6	6.5	15.2	Pan et al. [2011a]
Forests in U.S.	Inventory	2000–2007	257	147	57.2	14.4	7.0	78.6	18.3	27.2	Pan et al. [2011a]
Forests in Europe	Inventory	1990–1999	132.0	117	88.6	61.4	6.1	156.1	39.3	43.2	Pan et al. [2011a]
Forests in Europe	Inventory	2000–2007	144.5	137	94.8	45.0	5.5	145.3	31.0	34.8	Pan et al. [2011a]
Global forests	Meta-analysis[a]	1980–2000				15.2			15.2		Li et al. [2012]

[a]Data set contains 292 sites which come from 70 peer-reviewed papers.
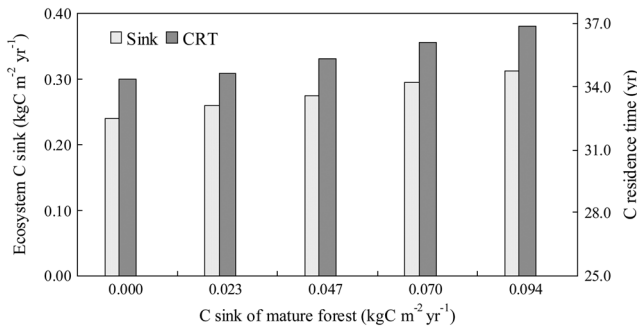
Figure 7. Sensitivities of nonsteady state of mature forest on the estimations of ecosystem carbon residence times (the first step) and carbon sink parameters (the second step).

[30] As allocation coefficients of NPP are dependent on forest age and environmental factors, we compared the estimated optimal NPP allocation parameters for mature forests (steady state sites only) with those for all forests (both steady and nonsteady state sites). The results indicated that forests have a higher NPP allocation to wood at nonsteady state ($\alpha_W = 0.52$) than at steady state ($\alpha_W = 0.42$), and accordingly a lower NPP allocation to leaves (0.37 versus 0.45).

[31] The NPP allocation to roots also differs between mature and immature sites; the allocation coefficient (ξ_{R1}) to the topsoil layer (0–20 cm) is higher at nonsteady state than at steady state (0.55 versus 0.50). Accordingly, the allocations to the second (ξ_{R2}) and third layers (ξ_{R3}) at nonsteady state are relatively lower (0.32 versus 0.35 and 0.12 versus 0.15, respectively).

3.3. Magnitudes and Uncertainties of Carbon Sink

[32] We summarized the magnitudes of the vegetation and soil carbon sink based on the optimal carbon sink parameters of 10 carbon pools and the map of vegetation type (Table 2). The results indicated that all the five forest types in China have net carbon uptakes in vegetation (leaves, stem, and roots). The average forest carbon sink in China is $89.74 \pm 16.82\,\mathrm{gC\,m^{-2}\,yr^{-1}}$, with the highest carbon sink for evergreen broadleaf forests ($215.41 \pm 19.30\,\mathrm{gC\,m^{-2}\,yr^{-1}}$) and the lowest carbon sink for mixed forests ($36.20 \pm 21.80\,\mathrm{gC\,m^{-2}\,yr^{-1}}$). When forest area was considered, we estimated the total forest carbon sink in China to be $117.2 \pm 22.0\,\mathrm{TgC\,yr^{-1}}$ (Table 3).

[33] Comparison of the carbon sink values determined in this study with the literatures (Table 3) indicated that our estimate of the vegetation carbon sink is comparable with those estimates mainly based on forest inventory data and with process-based models that considered detailed land use and land cover changes. Comparisons of forest carbon sinks in different geographic regions showed in Table 4, which indicates that the intensity of the vegetation carbon sink for China's forests ($89.74\,\mathrm{gC\,m^{-2}\,yr^{-1}}$) is similar to those of European forests, but significantly higher than the carbon sink in the U.S. and the global mean value.

[34] Soil carbon sink is positive in most of the forest types (i.e., EBF, DBF, DNF, and MF), except for evergreen needleleaf forest (ENF), which act as a carbon source at $14.65 \pm 19.10\,\mathrm{gC\,m^{-2}\,yr^{-1}}$ (Table 2). Among those forests, deciduous broadleaf forests and mixed forests are the largest carbon sinks, with yearly net soil carbon uptakes of $50.10 \pm 17.80\,\mathrm{gC\,m^{-2}\,yr^{-1}}$ and $41.84 \pm 13.10\,\mathrm{gC\,m^{-2}\,yr^{-1}}$, respectively. Evergreen broadleaf forests exhibit moderate uptake ($15.75 \pm 32.60\,\mathrm{gC\,m^{-2}\,yr^{-1}}$), while deciduous needleleaf forests have low carbon sinks ($1.55 \pm 26.80\,\mathrm{gC\,m^{-2}\,yr^{-1}}$).

[35] The average magnitude of soil carbon sink in China's forests is $14.06 \pm 20.65\,\mathrm{gC\,m^{-2}\,yr^{-1}}$, accounting for 13.0% of the total carbon sink ($108.5 \pm 28.67\,\mathrm{gC\,m^{-2}\,yr^{-1}}$) of the ecosystem (Table 3). Considering the carbon sink of the litter ($4.73 \pm 6.50\,\mathrm{gC\,m^{-2}\,yr^{-1}}$), soil and litter together account for 17.3% of the total carbon sink of the ecosystem.

[36] The comparisons between China's soil and vegetation indicated that although soil has a smaller average carbon sink magnitude and ratio (Table 2), it has a higher standard deviation ($20.65\,\mathrm{gC\,m^{-2}\,yr^{-1}}$ for soil compared with $16.82\,\mathrm{gC\,m^{-2}\,yr^{-1}}$ for vegetation). This higher uncertainty of soil carbon sink estimation is likely due to the higher uncertainties of model parameters that directly determine soil carbon sink, such as much higher variations in the optimal parameters of soil carbon residence time (Figure 5). In addition, change in soil carbon stock is controlled by more processes, and therefore, much more uncertainty is transmitted from upstream processes.

3.4. Sensitivity of Steady State Assumption on Parameter Estimation

[37] The sensitivity analysis indicated that when the carbon sinks of the mature forest were 0%, 2.5%, 5.0%, 7.5%, and 10.0% of the NPP, the estimated carbon residence times (the first step) were 34.35, 34.62, 35.36, 36.10, and 36.89 years, respectively, while the estimated carbon sinks (the second step) were 240, 259, 275, 296, and $312\,\mathrm{gC\,m^{-2}\,yr^{-1}}$, respectively (Figure 7). Thus, a higher carbon sink value for the mature forest is correlated with a higher ecosystem carbon residence time and, therefore, a lower carbon efflux and a higher carbon sink potential. Given that a mature forest is probably a small carbon sink [*Wharton et al.*, 2012], the magnitude of the carbon sink estimated from the steady state assumption was probably underestimated to some degree.

4. Discussion

4.1. Comparison of Two-Step and One-Step Approach

[38] We used the two-step approach, instead of the one-step approach (i.e., estimating all of the model parameters simultaneously), to estimate the carbon sink parameters based on the following considerations. (1) The one-step approach is relatively simple in its conception, but it is problematic during operation because most parameter estimation studies have showed that the number of parameters constrained by the observation data sets is limited, typically from a couple of parameters to less than 20 parameters [*Braswell et al.*, 2005; *Liu et al.*, 2008; *Wang et al.*, 2001; *Xu et al.*, 2006; *Yuan et al.*, 2012]. If the one-step approach is applied, 32 model parameters are estimated simultaneously, and it is difficult to guarantee their validity and reliability. (2) To increase the number of well-constrained parameters, more information is necessary to observations and models [*Wang et al.*, 2009]. The baseline carbon residence times are dependent mainly on the biome type [*Barrett*, 2002] and are usually regarded as invariable parameters in most biogeochemical models [*Kuppel et al.*, 2012], so the values of the estimated carbon sink parameters will be more reliable if the baseline carbon residence times are known.
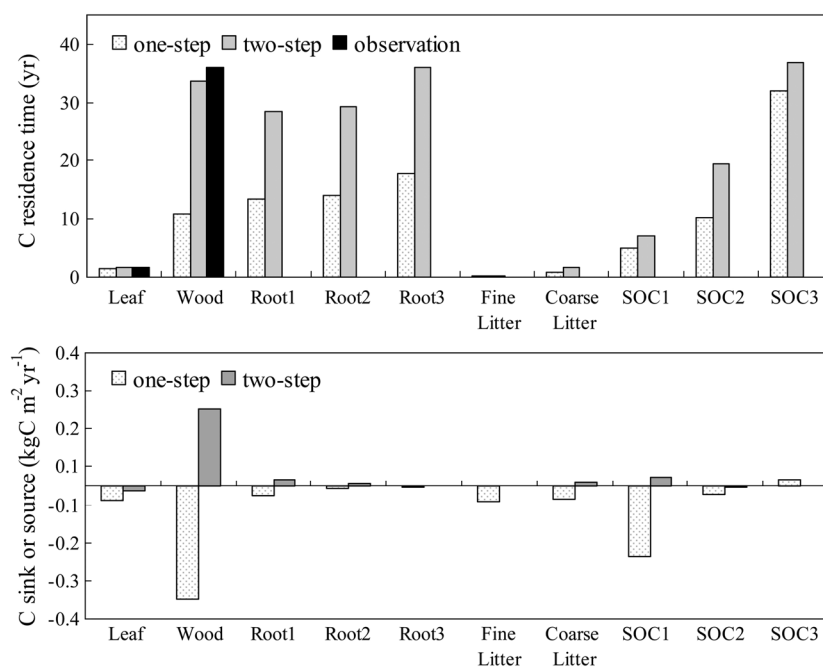
Figure 8. Comparison of estimated carbon residence times and carbon sink parameters between one-step and two-step approach.

Previous studies have indicated that the baseline carbon residence time parameters could be estimated based on the inverse of the observations of mature forests, where the carbon inputs and outputs are at or near a steady state [*Barrett*, 2002; *Zhou et al.*, 2010]. Thus, the two-step approach is theoretically necessary but also technically feasible because it solves the problem by estimating numerous unknown parameters if limited observational information is available.

[39] The comparisons between the two-step and the one-step approach indicated that when all of the mature and young forest observations were used simultaneously in the one-step approach, the values of carbon residence times were underestimated significantly (Figure 8). For example, the estimated residence times for stems and leaves using the one-step approach were only 10.91 and 1.43 years, respectively, which are significantly lower than the values (35.96 and 1.67 years, respectively) derived from field observations [*Luo*, 1996]. The poor estimates of the residence time of the wood pool using the one-step approach are similar to the results reported by *Fox et al.* [2009]. The underestimations of the carbon residence times with one-step approach lead to an overestimation of carbon efflux, which ultimately means that most of the carbon sink parameters will be negative (i.e., carbon sources). By contrast, the carbon residence times derived from the two-step approach were similar to the field observations [*Luo*, 1996], while the estimated carbon sink values agreed well with the values derived from the forest inventory and process-based models (Table 3).

[40] Overall, the results obtained using the one-step approach indicated that the limited observation information for the NPP, biomass, litter carbon, and SOC could not constrain the parameters of the carbon residence times effectively in a nonsteady state, which would significantly underestimate the values of the residence times and make the estimates of the carbon sink parameters meaningless. By contrast, the two-step approach utilizes the advantage of mature forest to estimate the carbon residence times and ensures that estimates of the carbon sink parameters are feasible.

4.2. Nonsteady State Modeling at Regional Scale

[41] Process-based models are widely applied in current studies for simulation and prediction of carbon sinks at nonsteady state. However, the estimated carbon sinks at the regional and global scales still have high uncertainties due to the improper model parameters, the lack of initial values of carbon pools, and the improper assumption of steady state [*Bellassen et al.*, 2011; *Carvalhais et al.*, 2008, 2010a; *Wang et al.*, 2011b].

[42] Carbon residence times are key model parameters that control carbon output, and therefore ultimately determine the value of the net flux (i.e., carbon sink) at nonsteady state [*Luo et al.*, 2003]. The carbon efflux in nearly all regional and global models is expressed as a function of carbon pool size and carbon residence time, which can be further expressed as the product of baseline residence times mainly determined by vegetation types and environmentally dependent scalars mainly determined by temperature and moisture [*Xia et al.*, 2013]. Although the baseline residence times are crucial for precise modeling of carbon dynamics, their values in regional carbon cycle models are often determined either arbitrarily or based on a few experiments or site observations. Few regional or global models systematically optimize those parameters before simulating the carbon dynamics.

[43] In this study, we estimated the optimal baseline residence times before estimating regional carbon sinks. Considering that the estimation of parameters (i.e., baseline residence times), state variables (i.e., pool sizes), and carbon fluxes are mutually dependent, the estimation of baseline residence times at nonsteady state is difficult, and a lot of observation data are needed to constrain those correlated model parameters [*Luo et al.*, 2003]. As a result, the estimation of optimal baseline residence times at regional

scale is commonly based on a steady state assumption [*Barrett*, 2002; *Zhou and Luo*, 2008; *Zhou et al.*, 2012]. This steady state approach was also applied in our two-step data assimilation scheme, where the observations in mature forest sites were selected in the first step to retrieve the optimal parameters of baseline residence times.

[44] Another factor that troubles regional and global modelers is the spatially explicit values of initial carbon pools. At the regional scale, neither observations of initial carbon pools nor time series data are available for most spatial grids, so it is difficult to directly estimate the magnitude of disequilibrium at nonsteady state. As a result, nearly all regional or global models have to spin-up their models to a steady state to retrieve the spatial distribution of initial carbon pools and then iteratively simulate carbon fluxes at nonsteady state [*Carvalhais et al.*, 2010a; *Potter et al.*, 1993; *Tian et al.*, 2011; *Xia et al.*, 2012]. However, the initial carbon pools estimated from the spin-up process to steady state do not reflect the nature of dynamic disequilibrium in the real world [*Luo and Weng*, 2011] and thus significantly impact the modeled carbon sink at nonsteady state [*Bellassen et al.*, 2011].

[45] Recent studies indicated that the initialization of carbon pools is quite important to the ability of process-based models to simulate the nonsteady state carbon flux [*Bellassen et al.*, 2011; *Carvalhais et al.*, 2010a]. Due to high spatial differences in disturbance regimes [*Luo and Weng*, 2011], it is improper for all spatial grids to arrive at steady state simultaneously, as spin-up does. Accordingly, using a spatially explicit map of the growth stage to provide a spatially more precise initialization can significantly decrease the modeled error [*Bellassen et al.*, 2011]. Unfortunately, spatial forest succession data are quite scarce for most regions [*Pan et al.*, 2011b] and thus hampers the precise estimation of the initialization for ecosystem carbon pools and the subsequent modeling of nonsteady state carbon flux. One study indicated that making an unreasonable steady state assumption deteriorates model performance and increases model errors, while relaxing the steady state assumption leads to a 92% decrease in the normalized average error [*Carvalhais et al.*, 2008]. In other words, the disequilibrium of the nonsteady state simulated by regional models inevitably contains uncertainties that originate from initial values caused by the steady state assumption and subsequent disturbances.

[46] In this study, we directly estimate the regional carbon flux at nonsteady state by a data assimilation method from the large sample of biometric data that distributed extensively throughout the region, therefore avoiding the process of spin-up that implemented in most regional models. As demonstrated in this study, the state of disequilibrium (i.e., 10 carbon sink parameters) can be estimated from various biometric observations (i.e., NPP, biomass, litter, and SOC) with the two-step data assimilation scheme. In addition, the directly estimated disequilibrium in our study is likely to have less uncertainty, as it avoids some uncertainties associated from the initial values (i.e., most of information in this method is observation-based and few exogenous uncertainties are introduced).

[47] Because our data assimilation scheme is based on partial information available at various sites that is integrated to retrieve the general state at regional scale, it is only suitable for estimating the regional means of carbon sinks rather than for constructing a spatial grid as performed by most regional models. In addition, as the measurement times of

those different site observations are not exactly the same, the regional carbon sink estimate represents the mean over the data collection period.

4.3. Comparison of Carbon Sinks by Different Methods

[48] Comparisons of the carbon sink estimations in this study with estimates in the literature (Table 3) indicated that our estimated vegetation carbon sink is comparable with estimates based on forest inventory data, in which the estimated vegetation sink ranges from 43.1 to 147.1 gC m^{-2} yr^{-1} [*Fang et al.*, 2007; *Lun et al.*, 2012; *Pan et al.*, 2004, 2011a; *Wang et al.*, 2010], and with process-based models that consider detailed land use and changes in land cover [*Tian et al.*, 2011]. When forest area was considered, we estimated the total forest carbon sink in China as 117.2 ± 22.0 TgC yr^{-1} (Table 3).

[49] Forest carbon sinks were compared among different geographic regions (Table 4). The intensity of vegetation carbon sink in China's forests (89.74 gC m^{-2} yr^{-1}) is similar to those for European forests (88.6–94.8 gC m^{-2} yr^{-1}), but significantly higher than the carbon sink in the U.S. (48.0–57.2 gC m^{-2} yr^{-1}) and the global mean value (75.5–76.4 gC m^{-2} yr^{-1}). The relatively high vegetation carbon of China's forests was attributed to the higher than average proportion of young forests [*Fang et al.*, 2007], which have a higher NPP allocation coefficient to wood (Figure 6).

[50] In contrast to the consistent pattern that all studies have shown that vegetation is a carbon sink with somewhat different magnitudes, the estimates of soil carbon sinks in different studies differed greatly (i.e., carbon sinks in some studies but sources in others) and had the highest uncertainties in ecosystems [*Fang et al.*, 2007; *Huang et al.*, 2010; *Pan et al.*, 2011a].

[51] In this study, most forest soils have been estimated to exhibit net carbon uptake and deciduous broadleaf forests have the highest soil carbon sink (50.10 ± 17.80 gC m^{-2} yr^{-1}). This is consistent with the results of *Paul et al.* [2002], who summarized the literature on global forests and determined that deciduous forests exhibit the greatest accumulation of soil carbon. Our results indicated that evergreen needleleaf forest is the only forest type that exhibits net soil carbon efflux. The role of ENF as a carbon source depends on the characteristics of needleleaf forests [*Li et al.*, 2012] and the relative youth of forests in China [*Dai et al.*, 2011]. ENF in China is the main forest type for the national afforestation projects. The planted ENF, dominated by *Pinus tabulaeformis*, *P. massoniana*, *Cunninghamia spp.*, accounts for over 70% of total ENF in the country and were mostly planted in past 10–30 years. Meta-analyses indicated that the soil of young needleleaf forests (forage age < 30 years) worldwide exhibit net carbon release [*Li et al.*, 2012; *Paul et al.*, 2002; *Yang et al.*, 2011].

[52] This study estimated the carbon sink of soil in China's forests as 14.1 ± 20.7 gC m^{-2} yr^{-1}, which accounts for 13.0% of the total ecosystem carbon sink (Table 3). This ratio of 13.0% is similar to the value of 18.6% found by *Pan et al.* [2011a] using the forest inventory method and the value of 16.4% found by *Tian et al.* [2011] using the process-based model. The study based on meta-analysis indicated that global forests are generally carbon sinks, and the average soil sink is 15.2 gC m^{-2} yr^{-1} [*Li et al.*, 2012], similar to China's soil carbon (14.1 gC m^{-2} yr^{-1}). The comparison of the ratios of soil carbon sinks to the total ecosystem carbon sink (Table 4) indicated that the value in China (13.0%) is similar

to those of the global average values (12.8–13.7%), but smaller than regions of Europe (31.0–39.3%) and temperate forests (23.8–29.0%).

[53] As roots are deeper in mature forests than immature forests, the carbon allocation to the topsoil layer is greater in immature forests, leading to a higher carbon sink intensity of the topsoil layer (Figure 6), consistent with the meta-analysis results deduced from the observed changes in soil organic carbon [Li et al., 2012].

[54] The comparisons of soil carbon sinks among different geographic regions (Table 4) indicated that the soil carbon sink in China is similar to that in the U.S. ($14.4\,\mathrm{gC\,m^{-2}\,yr^{-1}}$) and slightly higher than the global mean (11.8–$12.6\,\mathrm{gC\,m^{-2}}$ $\mathrm{yr^{-1}}$), but much lower than in European forests (45.0–$61.4\,\mathrm{gC\,m^{-2}\,yr^{-1}}$). As for the carbon sink of the litter pool, most geographic regions (Table 4) have similar intensities in the range of 4.1 to $7.0\,\mathrm{gC\,m^{-2}\,yr^{-1}}$. China has a moderate litter carbon sink ($4.7\,\mathrm{gC\,m^{-2}\,yr^{-1}}$) that is slightly higher than the mean of global forests but lower than European (5.5–$6.1\,\mathrm{gC\,m^{-2}\,yr^{-1}}$) and American forests ($4.9$–$7.0\,\mathrm{gC\,m^{-2}\,yr^{-1}}$).

5. Conclusions

[55] In this study, we developed a two-step data assimilation scheme based on the large sample information of traditionally biometric observations and combined with the process-based model and remote sensing data to inversely estimate the mean regional carbon sink for China's forests. The results showed that the two-step scheme significantly increases the number of the well-estimated model parameters and matches modeled NPP, biomass, and SOC values well with observations. The magnitude of disequilibrium expressed by carbon sink parameters could be accurately estimated by the two-step data assimilation scheme. The results indicated that all forest types (EBF, DBF, ENF, DNF, and MF) in China exhibit net carbon uptake in vegetation, and the regional mean carbon sink size for vegetation pools is $89.7 \pm 16.8\,\mathrm{gC\,m^{-2}\,yr^{-1}}$. As for forest soil and litter, the results indicated that most forests (EBF, DBF, DNF, and MF) are carbon sinks, with the exception of ENF. The regional mean carbon sink sizes for soil and litter are $14.1 \pm 20.7\,\mathrm{gC\,m^{-2}\,yr^{-1}}$ and $4.7 \pm 6.5\,\mathrm{gC\,m^{-2}\,yr^{-1}}$, respectively, accounting for 13.0% and 4.3% of the total ecosystem carbon sink ($108.5 \pm 28.7\,\mathrm{gC\,m^{-2}\,yr^{-1}}$). These results showed that the general characteristics (e.g., means) of regional carbon sinks can be directly derived from the large available sample of traditional ecological observations, despite the spatial discontinuity and incomplete information at sites with the data assimilation scheme is designed to combine this information with model information and spatially continuous auxiliary information (i.e., remote sensing and GIS data).

Appendix A: Model Description

[56] The data assimilation conducted in this study was based on a Terrestrial Ecosystem Regional (TECO-R) model (Figure 2), which was developed by combining CASA light-use efficiency model [Field et al., 1995; Potter et al., 1993] and the Vegetation And Soil Carbon Transfer (VAST) model [Barrett, 2002]. The TECO-R model divided root biomass and soil organic carbon (SOC) into three soil layers (top: 0–20 cm, middle: 20–50 cm, and bottom: 50–100 cm). As the TECO-R model depicts the basic processes of carbon transfer

among pools, its model structure is suitable for all forest ecosystems when appropriate model parameters that reflect forest-specific characteristics are applied. The key model parameters in the TECO-R model include the maximum light-use efficiency (ε^*), NPP allocation among leaves, stem, and roots (α_L, α_W, α_R, ξ_{R1}, ξ_{R2}, and ξ_{R3}), carbon partition coefficients (θ_F, θ_C, η, θ_{S_1}, and θ_{S_2}), and baseline residence times in individual plant and soil pools $\left(\tau_L, \tau_W, \tau_{R_1}, \tau_{R_2}, \tau_{R_3}, \tau_F^*, \tau_C^*, \tau_{S_1}^*, \tau_{S_2}^*, \mathrm{and}\, \tau_{S_3}^*\right)$. Table 1 lists detailed information on those model parameters.

[57] The actual carbon residence times of litter and SOC pools ($\tau_F, \tau_C, \tau_{S_1}, \tau_{S_2}, \mathrm{and}\, \tau_{S_3}$) are affected by climate factors, soil properties, and vegetation types. The decomposition rates of litter and soil organic matter are controlled primarily by the properties of soil microbes, which are closely related to site-specific climate factors and soil properties. Forest type also significantly impacts carbon residence times. On the one hand, plant tissues (i.e., leaves, stems, and roots pools) of different forest types exhibit differences in residence times. Litters (i.e., fine litter and coarse litter pools) of different forests also have different chemical compositions (e.g., the ratio of lignin to nitrogen), which affects the decomposition rates of litter pools [Potter et al., 1993]. To reflect the potential influence of forest type on parameter estimation, the TECO-R model divided Chinese forests into five types based on a 1:400 M vegetation map: evergreen broadleaf forest (EBF), deciduous broadleaf forest (DBF), evergreen needleleaf forest (ENF), deciduous needleleaf forest (DNF), and mixed forest (MF). The optimal model parameters were estimated separately for different forest types. To quantify potential influences caused by the spatial heterogeneity of climate factors, the TECO-R model relates site-specific residence times ($\tau_F, \tau_C, \tau_{S_1}, \tau_{S_2}, \mathrm{and}\, \tau_{S_3}$) to the baseline residence times determined by vegetation type $\left(\tau_F^*, \tau_C^*, \tau_{S_1}^*, \tau_{S_2}^*, \mathrm{and}\, \tau_{S_3}^*\right)$ by

$$\tau_k = \tau^*_k / (W_s \cdot T_s), \qquad k = F, C, S_1, S_2, S_3, \qquad (A1)$$

where τ_k and τ^*_k are the actual residence time and baseline residence time, respectively, for fine litter (F), coarse litter (C), and three soil carbon pools (S_1, S_2, and S_3); and W_s and T_s are the temperature and moisture scalars for site-specific carbon residence times. The moisture scalar (W_s) is estimated by monthly precipitation (PPT), potential evapotranspiration (PET), and soil moisture (SoilM) simulated by the CASA soil moisture submodel [Randerson et al., 1996]:

$$SM = \frac{PPT + SoilM}{PET} \qquad (A2)$$

$$W_s = 0.1 + 0.9 \cdot SM \qquad 0 \le SM \le 1 \qquad (A3)$$

$$W_s = 1.0 \qquad 1 < SM \le 2 \qquad (A4)$$

$$W_s = [1.0 + (1.0/28.0)] - (0.5/28.0)SM \qquad 2 < SM \le 30 \qquad (A5)$$

$$W_s = 0.5 \qquad 30 \le SM. \qquad (A6)$$

[58] The temperature scalar of decomposition, T_s, was obtained directly from monthly temperature data (T), as in the Century soil carbon model [*Parton et al.*, 1987]:

$$T_s = \begin{cases} 1/(1 + 19e^{-0.16T}), & T < 45°C \\ 10 - 0.2T, & 45 \le T \le 50°C \,. \\ 0, & T > 50°C \end{cases} \quad (A7)$$

Appendix B: NPP Modeling and Allocation

[59] In the TECO-R model, NPP is a function of the absorbed photosynthetically active radiation (APAR), maximum light-use efficiency (ε^*), and temperature and moisture stress scalars (T_ε, W_ε).

$$NPP = f APAR \cdot PAR \cdot \varepsilon^* \cdot T_\varepsilon \cdot W_\varepsilon, \quad (B1)$$

where fAPAR is the fraction of PAR that is absorbed by vegetation and is determined using a linear relationship with normalized difference vegetation index (NDVI). Thus, APAR equals fAPAR times PAR. PAR is estimated by observed solar radiation (Sr), i.e., PAR = Sr × 0.5. In the TECO-R model, we used the same scalars as the CASA model for T_ε and W_ε [*Randerson et al.*, 1996].

[60] The estimated total NPP is allocated to the plant tissues of leaves, stem, and roots according to the carbon allocation coefficients:

$$NPP_L = \alpha_L \times NPP \quad (B2)$$

$$NPP_W = \alpha_W \times NPP \quad (B3)$$

$$NPP_R = \alpha_R \times NPP, \quad (B4)$$

where α_L, α_W, α_R are the NPP allocation coefficients for leaves, wood, and roots, respectively.

Appendix C: Carbon Pools at Steady State

[61] Given the carbon input in Appendix B, the modeled carbon pools of leaves, stems, and roots at steady state can be described by

$$q_L = NPP_L \times \tau_L \quad (C1)$$

$$q_W = NPP_W \times \tau_W \quad (C2)$$

$$q_{R1} = \xi_{R1} \times NPP_R \times \tau_{R1} \quad (C3)$$

$$q_{R2} = \xi_{R2} \times NPP_R \times \tau_{R2} \quad (C4)$$

$$q_{R3} = \xi_{R3} \times NPP_R \times \tau_{R3}, \quad (C5)$$

where q_L, q_W, q_{R1}, q_{R2}, and q_{R3} are the sizes of carbon pools in leaves, wood, and roots for three soil layers (0–20 cm, 20–50 cm, and 50–100 cm), respectively; τ_L, τ_W, τ_{R1}, τ_{R2}, and τ_{R3} are the carbon residence times for the corresponding pools; and ξ_{R1}, ξ_{R2}, and ξ_{R3} are the allocation proportion to roots at three layers.

[62] The carbon pool sizes in the litter and soil organic carbon (SOC) are determined by the amount of carbon transferred from the plant biomass and can be modeled by

$$q_C = q_W/\tau_W \times \tau_C \quad (C6)$$

$$q_F = (q_L/\tau_L + \eta \times q_C/\tau_C) \times \tau_F \quad (C7)$$

$$q_{S1} = (q_{R1}/\tau_{R1} + \theta_F \times q_F/\tau_F + \theta_C \times q_C/\tau_C) \times \tau_{S1} \quad (C8)$$

$$q_{S2} = (q_{R2}/\tau_{R2} + \theta_{S1} \times q_{S1}/\tau_{S1}) \times \tau_{S2} \quad (C9)$$

$$q_{S3} = (q_{R3}/\tau_{R3} + \theta_{S2} \times q_{S2}/\tau_{S2}) \times \tau_{S3}, \quad (C10)$$

where q_F and q_C are the carbon pool sizes for fine and coarse litter, respectively; q_{S_1}, q_{S_2}, and q_{S_3} are the pool sizes of SOC in the three soil layers; τ_F, τ_C, τ_{S_1}, τ_{S_2}, and τ_{S_3} are the carbon residence times in fine litter, coarse litter, and the SOC in the three layers, respectively; η is the fraction of C exiting the coarse woody debris pool by mechanical breakdown; θ_F and θ_C are the carbon partitioning coefficients of the fine litter and coarse litter pools, respectively; and θ_{S_1} and θ_{S_2} are the partition coefficients of SOC in the first and second soil layers, respectively.

Appendix D: Carbon Pools at Nonsteady State

[63] When the carbon cycle processes of an ecosystem are at nonsteady state then the carbon input for a certain pool does not equal the carbon output, controlled by its pool size and residence time. To precisely simulate the carbon pools, additional parameters that describe the intensity of the disequilibrium are required (i.e., the net flux of the input and output). As a result, the modeled carbon pools for leaves, stems, and roots at nonsteady state can be described by

$$q_L = (NPP_L - \Delta_L) \times \tau_L \quad (D1)$$

$$q_W = (NPP_W - \Delta_W) \times \tau_W \quad (D2)$$

$$q_{R1} = (\xi_{R1} \times NPP_R - \Delta_{R1}) \times \tau_{R1} \quad (D3)$$

$$q_{R2} = (\xi_{R2} \times NPP_R - \Delta_{R2}) \times \tau_{R2} \quad (D4)$$

$$q_{R3} = (\xi_{R3} \times NPP_R - \Delta_{R3}) \times \tau_{R3}, \quad (D5)$$

where Δ_L, Δ_W, Δ_{R1}, Δ_{R2}, and Δ_{R3} are the carbon sink parameters (i.e., the net flux of input minus output) for leaf, stem, and root carbon pools, where positive parameter values denote carbon sinks (i.e., carbon input greater than output for a certain pool) and negative parameter values denote carbon sources (i.e., net carbon release). Similarly, the carbon pool sizes in the litter and soil organic carbon (SOC) can be described by

$$q_C = (q_W/\tau_W - \Delta_C) \times \tau_C \quad (D6)$$

$$q_F = (q_L/\tau_L + \eta \times q_C/\tau_C - \Delta_F) \times \tau_F \quad (D7)$$

$$q_{S1} = (q_{R1}/\tau_{R1} + \theta_F \times q_F/\tau_F + \theta_C \times q_C/\tau_C - \Delta_{S1}) \times \tau_{S1} \quad (D8)$$

$$q_{S2} = (q_{R2}/\tau_{R2} + \theta_{S1} \times q_{S1}/\tau_{S1} - \Delta_{S2}) \times \tau_{S2} \quad (D9)$$

$$q_{S3} = (q_{R3}/\tau_{R3} + \theta_{S2} \times q_{S2}/\tau_{S2} - \Delta_{S3}) \times \tau_{S3}, \quad (D10)$$

where Δ_C, Δ_F, Δ_{S1}, Δ_{S2}, and Δ_{S3} are the carbon sink parameters for coarse litter, fine litter, and three soil layers, with positive values indicating carbon sinks (net gain) and negative values indicating carbon sources (net release).

References

Baldocchi, D., et al. (2001), FLUXNET: A new tool to study the temporal and spatial variability of ecosystem-scale carbon dioxide, water vapor, and energy flux densities, *Bull. Am. Meteorol. Soc.*, *82*, 2415–2434.

Ballantyne, A. P., C. B. Alden, J. B. Miller, P. P. Tans, and J. W. C. White (2012), Increase in observed net carbon dioxide uptake by land and oceans during the past 50 years, *Nature*, *488*, 70–73.

Barrett, D. J. (2002), Steady state turnover time of carbon in the Australian terrestrial biosphere, *Global Biogeochem. Cycles*, *16*(4), 1108, doi:10.1029/2002GB001860.

Bellassen, V., N. Delbart, G. Le Maire, S. Luyssaert, P. Ciais, and N. Viovy (2011), Potential knowledge gain in large-scale simulations of forest carbon fluxes from remotely sensed biomass and height, *For. Ecol. Manage.*, *261*, 515–530.

Braswell, B. H., W. J. Sacks, E. Linder, and D. S. Schimel (2005), Estimating diurnal to annual ecosystem parameters by synthesis of a carbon flux model with eddy covariance net ecosystem exchange observations, *Global Change Biol.*, *11*, 335–355.

Carvalhais, N., et al. (2008), Implications of the carbon cycle steady state assumption for biogeochemical modeling performance and inverse parameter retrieval, *Global Biogeochem. Cycles*, *22*, GB2007, doi:10.1029/2007GB003033.

Carvalhais, N., M. Reichstein, P. Ciais, G. J. Collatz, M. D. Mahecha, L. Montagnani, D. Papale, S. Rambal, and J. Seixas (2010a), Identification of vegetation and soil carbon pools out of equilibrium in a process model via eddy covariance and biometric constraints, *Global Change Biol.*, *16*, 2813–2829.

Carvalhais, N., M. Reichstein, G. J. Collatz, M. D. Mahecha, M. Migliavacca, C. S. R. Neigh, E. Tomelleri, A. A. Benali, D. Papale, and J. Seixas (2010b), Deciphering the components of regional net ecosystem fluxes following a bottom-up approach for the Iberian Peninsula, *Biogeosciences*, *7*, 3707–3729.

Chen, P. Q., X. K. Wang, L. M. Wang (2008), *Carbon Budgets of Terrestrial Ecosystems and Countermeasures to Achieve Carbon Sink in China* (in Chinese), Science Press, Beijing.

Dai, M., T. Zhou, L. Yang, and G. Jia (2011), Spatial pattern of forest ages in China retrieved from national-level inventory and remote sensing imageries (in Chinese), *Geogr. Res.*, *30*, 172–184.

Fang, J. Y., Z. D. Guo, S. L. Piao, and A. P. Chen (2007), Terrestrial vegetation carbon sinks in China, 1981–2000, *Sci. China Earth Sci.*, *50*, 1341–1350.

Field, C. B., J. T. Randerson, and C. M. Malmstrom (1995), Global net primary production: Combining ecology and remote sensing, *Remote Sens. Environ.*, *51*, 74–88.

Fox, A., et al. (2009), The REFLEX project: Comparing different algorithms and implementations for the inversion of a terrestrial ecosystem model against eddy covariance data, *Agric. For. Meteorol.*, *149*, 1597–1615.

Friedlingstein, P., et al. (2006), Climate–carbon cycle feedback analysis: Results from the C4MIP Model Intercomparison, *J. Clim.*, *19*, 3337–3353.

Huang, Y., W. J. Sun, W. Zhang, and Y. Yu (2010), Changes in soil organic carbon of terrestrial ecosystems in China: A mini-review, *Sci. China Life Sci.*, *53*, 766–775.

Intergovernmental Panel on Climate Change (2007), *Climate Change 2007: The Physical Science Basis*, Cambridge Univ. Press, New York.

Kuppel, S., P. Peylin, F. Chevallier, C. Bacour, F. Maignan, and A. D. Richardson (2012), Constraining a global ecosystem model with multi-site eddy-covariance data, *Biogeosciences*, *9*, 3757–3776.

Li, X., T. Zhou, and X. He (2009), Carbon sink of forest ecosystem driven by NPP increasing in China (in Chinese), *J. Nat. Resour.*, *24*, 491–497.

Li, D. J., S. Niu, and Y. Luo (2012), Global patterns of the dynamics of soil carbon and nitrogen stocks following afforestation: A meta-analysis, *New Phytol.*, *195*, 172–181.

Liu, S. (2009), Quantifying the spatial details of carbon sequestration potential and performance, in *Carbon Sequestration and Its Role in the Global Carbon Cycle*, Geophys. Monogr. Ser., vol. *183*, edited by B. J. McPherson, and E. T. Sundquist, pp. 117–128, AGU, Washington, D. C., doi:10.1029/2006GM000524.

Liu, S., P. Anderson, G. Zhou, B. Kauffman, F. Hughes, D. Schimel, V. Watson, and J. Tosi (2008), Resolving model parameter values from carbon and nitrogen stock measurements in a wide range of tropical mature forests using nonlinear inversion and regression trees, *Ecol. Modell.*, *219*, 327–341.

Lun, F., W. Li, and Y. Liu (2012), Complete forest carbon cycle and budget in China, 1999–2008, *For. Ecol. Manage.*, *264*, 81–89.

Luo, T. X. (1996), Patterns of net primary productivity for Chinese major forest types and its mathematical models (in Chinese), Doctoral Dissertation, Institute of Geographic Sciences and Natural Resources Research, CAS, Beijing.

Luo, Y., and E. Weng (2011), Dynamic disequilibrium of terrestrial carbon cycle under global change, *Trends Ecol. Evol.*, *26*, 96–104.

Luo, Y., L. White, J. G. Canadell, E. H. DeLucia, D. S. Ellsworth, A. Finzi, J. Lichter, and W. H. Schlesinger (2003), Sustainability of terrestrial carbon sequestration: A case study in Duke Forest with inversion approach, *Global Biogeochem. Cycles*, *17*(1), 1021, doi:10.1029/2002GB001923.

Luo, Y., K. Ogle, C. Tucker, S Fei, C. Gao, S. LaDeau, J. S. Clark, and D. S. Schimel (2011), Ecological forecasting and data assimilation in a data-rich era, *Ecol. Appl.*, *21*, 1429–1442.

Pan, Y., T. Luo, R. Birdsey, J. Hom, and J. Melillo (2004), New estimates of carbon storage and sequestration in China's forests: Effects of age-class and method on inventory-based carbon estimation, *Clim. Change*, *67*, 211–236.

Pan, Y., et al. (2011a), A large and persistent carbon sink in the world's forests, *Science*, *333*, 988–993.

Pan, Y., J. M. Chen, R. Birdsey, K. McCullough, L. He, and F. Deng (2011b), Age structure and disturbance legacy of North American forests, *Biogeosciences*, *8*, 715–732.

Parton, W. J., D. S. Schimel, C. V. Cole, and D. S. Ojima (1987), Analysis of factors controlling soil organic matter levels in Great Plains grasslands, *Soil Sci. Soc. Am. J.*, *51*, 1173–1179.

Paul, K. I., P. J. Polglase, J. G. Nyakuengama, and P. K. Khanna (2002), Change in soil carbon following afforestation, *For. Ecol. Manage.*, *168*, 241–257.

Piao, S. L., J. Y. Fang, L. M. Zhou, B. Zhu, K. Tan, and S. Tao (2005), Changes in vegetation net primary productivity from 1982 to 1999 in China, *Global Biogeochem. Cycles*, *19*, GB2027, doi:10.1029/2004GB002274.

Piao, S. L., J. Y. Fang, P. Ciais, P. Peylin, Y. Huang, S. Sitch, and T. Wang (2009), The carbon balance of terrestrial ecosystems in China, *Nature*, *458*, 1009–1013.

Potter, C. S., J. T. Randerson, C. B. Field, P. A. Matson, P. M. Vitousek, H. A. Mooney, and S. A. Klooster (1993), Terrestrial ecosystem production: A process model based on global satellite and surface data, *Global Biogeochem. Cycles*, *7*, 811–841.

Randerson, J. T., M. V. Thompson, C. M. Malmstrom, C. B. Field, and I. Y. Fung (1996), Substrate limitations for heterotrophs: Implications for models that estimate the seasonal cycle of atmospheric CO2, *Global Biogeochem. Cycles*, *10*, 585–602.

Sarmiento, J. L., M. Gloor, N. Gruber, C. Beaulieu, A. R. Jacobson, S. M. Fletcher, S. Pacala, and K. Rodgers (2010), Trends and regional distributions of land and ocean carbon sinks, *Biogeosciences*, *7*, 2351–2367.

Tian, H., et al. (2011), China's terrestrial carbon balance: Contributions from multiple global change factors, *Global Biogeochem. Cycles*, *25*, GB1007, doi:10.1029/2010GB003838.

Wang, Y. P., R. Leuning, H. A. Cleugh, and P. A. Coppin (2001), Parameter estimation in surface exchange models using non-linear inversion: How many parameters can we estimate and which measurements are most useful?, *Global Change Biol.*, *7*, 495–510.

Wang, S., H. Tian, J. Liu, and S. Pan (2003), Pattern and change of soil organic carbon storage in China: 1960s–1980s, *Tellus B*, *55*, 416–427.

Wang, Y. P., C. M. Trudinger, and I. G. Enting (2009), A review of applications of model–data fusion to studies of terrestrial carbon fluxes at different scales, *Agric. For. Meteorol.*, *149*, 1829–1842.

Wang, B., J. Huang, X. Yang, B. Zhang, and M. Liu (2010), Estimation of biomass, net primary production and net ecosystem production of China's forests based on the 1999–2003 National Forest Inventory, *Scand. J. For. Res.*, *25*, 544–553.

Wang, S., L. Zhou, J. Chen, W. Ju, X. Feng, and W. Wu (2011a), Relationships between net primary productivity and stand age for several forest types and their influence on China's carbon balance, *J. Environ. Manage.*, *92*, 1651–1662.

Wang, W., J. Dungan, H. Hashimoto, A. R. Michaelis, C. Milesi, K. Ichii, and R. R. Nemani (2011b), Diagnosing and assessing uncertainties of terrestrial ecosystem models in a multimodel ensemble experiment: 1. Primary production, *Global Change Biol.*, *17*, 1350–1366.

Weng, E., and Y. Luo (2011), Relative information contributions of model vs. data to constraints of short- and long-term forecasts of forest carbon dynamics, *Ecol. Appl.*, *21*, 1490–1505.

Wharton, S., M. Falk, K. Bible, M. Schroeder, and K. T. Paw U (2012), Old-growth CO2 flux measurements reveal high sensitivity to climate anomalies across seasonal, annual and decadal time scales, *Agric. For. Meteorol.*, *161*, 1–14.

White, L., and Y. Luo (2002), Inverse analysis for estimating carbon transfer coefficients in Duke Forest, *Appl. Math. Comput.*, *130*, 101–120.

Wilks, D. S. (2006), *Statistical Methods in the Atmospheric Science*, pp. 166–170, Academic Press, San Diego.

Williams, C. A., G. J. Collatz, J. Masek, and S. N. Goward (2012), Carbon consequences of forest disturbance and recovery across the conterminous United States, *Global Biogeochem. Cycles*, *26*, GB1005, doi:10.1029/2010GB003947.

Xia, J., Y. Luo, Y. Wang, E. Weng, and O. Hararuk (2012), A semi-analytical solution to accelerate spin-up of coupled carbon and nitrogen land models to steady states, *Geosci. Model Dev.*, *5*, 1259–1271, doi:10.5194/gmd-5-1259-2012.

Xia, J., Y. Luo, Y. Wang, and O. Hararuk (2013), Traceable components of terrestrial carbon storage capacity in biogeochemical models, *Global Change Biol.*, *19*, 2104–2116.

Xiao, J., K. J. Davis, N. M. Urban, K. Keller, and N. Z. Saliendra (2011), Upscaling carbon fluxes from towers to the regional scale: Influence of parameter variability and land cover representation on regional flux estimates, *J. Geophys. Res.*, *116*, G00J06, doi:10.1029/2010JG001568.

Xie, Z. B., J. G. Zhu, G. Liu, G. Cadisch, T. Hasegawa, C. Chen, H. Sun, H. Tang, and Q. Zeng (2007), Soil organic carbon stocks in China and changes from 1980s to 2000s, *Global Change Biol.*, *13*, 1989–2007.

Xu, T., L. White, D. Hui, and Y. Luo (2006), Probabilistic inversion of a terrestrial ecosystem model: Analysis of uncertainty in parameter estimation and model prediction, *Global Biogeochem. Cycles*, *20*, GB2007, doi:10.1029/2005gb002468.

Yang, Y. H., Y. Luo, and A. C. Finzi (2011), Carbon and nitrogen dynamics during forest stand development: A global synthesis, *New Phytol.*, *190*, 977–989.

Yuan, W., et al. (2007), Deriving a light use efficiency model from eddy covariance flux data for predicting daily gross primary production across biomes, *Agric. For. Meteorol.*, *143*, 189–207.

Yuan, W., S. Liang, S. Liu, E. Weng, Y. Luo, D. Hollinger, and H. Zhang (2012), Improving model parameter estimation using coupling relationships between vegetation production and ecosystem respiration, *Ecol. Modell.*, *240*, 29–40.

Zhang, F., J. Chen, J. Chen, C. M. Gough, T. A. Martin, and D. Dragoni (2012), Evaluating spatial and temporal patterns of MODIS GPP over the conterminous U.S. against flux measurements and a process model, *Remote Sens. Environ.*, *124*, 717–729.

Zhao, M., and S. Running (2010), Drought-induced reduction in global terrestrial net primary production from 2000 through 2009, *Science*, *329*, 940–943.

Zhou, T., and Y. Luo (2008), Spatial patterns of ecosystem carbon residence time and NPP-driven carbon uptake in the conterminous United States, *Global Biogeochem. Cycles*, *22*, GB3032, doi:10.1029/2007GB002939.

Zhou, T., P. Shi, G. Jia, X. Li, and Y. Luo (2010), Spatial patterns of ecosystem carbon residence time in Chinese forests, *Sci. China Earth Sci.*, *53*, 1091–1248.

Zhou, X., T. Zhou, and Y. Luo (2012), Uncertainties in carbon residence time and NPP-driven carbon uptake in terrestrial ecosystems of the conterminous USA: A Bayesian approach, *Tellus B*, *64*, 17,223, doi:10.3402/tellusb.v64i0.17223.